

# Theoretical and Experimental Investigations Concerning the Fluorescence of some Azaheterocycles

---

## PhD Thesis Abstract

*Institution:* University "Alexandru Ioan Cuza" of Iasi, Romania

*Candidate:* Dan Maftai

*Scientific advisor:* Prof. Ionel I. Mangalagiu, PhD

---

## Introduction and objectives

Photophysics of five- and six-membered ring aromatic azaheterocycles is dominated by low-lying excited states involving electron promotion either to diffuse  $\sigma^*$  N-H antibonding orbitals (in acidic pyrrole and imidazole [1–4]) or from nitrogen lone-pairs orbitals ( $n\pi^*$  states in pyridine and all the three diazines, respectively [5–8]). Consequently, most of these molecules lack the efficient fluorescence emission required for practical applications.

Both types of nonradiative deactivation channels are suppressed in indolizine, a N-bridgehead 5,6-fused ring heterocycle derived formally from pyrrole and pyridine (see Figure 1). Unsubstituted indolizine, as well as the few

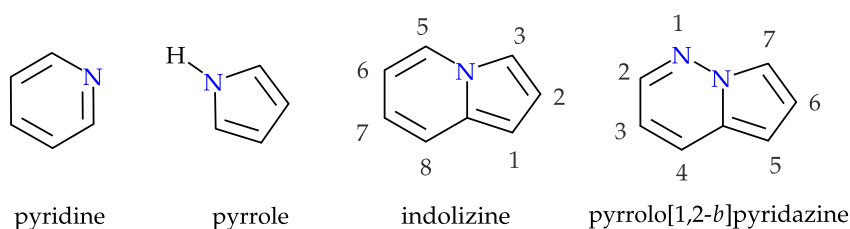


**Figure 1** – Structures of pyridine, pyrrole, indolizine and pyrrolo[1,2-*b*]pyridazine (5-azaindolizine)

azaindolizines for which photophysical properties were reported in the literature during the mid 70's [9–11], exhibit highly efficient fluorescence emission in the near-UV spectral region.

More recent experimental works on functionalized indolizine and pyrrolo[1,2-*b*]pyridazine show that the emission properties of the heterocycle are preserved by some functional groups, whereas others impact on fluorescence

emission, apparently in an unsystematic fashion [12–17]. In case of the former, potential applications areas suggested by several authors include optoelectronic devices [12] (provided the blue fluorescent emission of pyrrolo[1,2-*b*]pyridazine derivatives), chemical sensors [18] (by pH- [19,20] and solvent-dependent spectral shifts) etc.

Although few previous attempts in rationalizing the optical spectral properties of indolizines exist, none has accounted the entire picture and only few addressed different aspects with satisfactory results.

The first theoretical approaches [21,22] were based on heavily-parametrized SCF methods (either Hückel or Pariser–Par–Popple) and are therefore susceptible to give biased results when extrapolated to larger systems.

None of the more recent theoretical studies [23–25] has gone beyond the vertical approximation in computing the electronic spectra, whereas for these systems it is shown in the present work that modeling the vibronic band shape is crucial for assessing the accuracy of various density functionals.

Solvent effects in the few previous TD-DFT studies on (aza)indolizine derivatives were accounted in the simple but unphysical linear-response formalism (LR-PCM) that predicts solvatochromic shifts in qualitative contrast with experiment. Finally, none of the previous approaches by other authors has attempted to rationalize the effects of substitution based on the nature and the energetics of the corresponding excited state in the unsubstituted heterocycle.

Given the recent interest in exploiting the fluorescence emission of (aza)indolizine for practical applications, original contributions brought by this thesis attempt to rationalize the influence of substitution on their near-UV/Vis spectra. To this end, for the first time *first principles* theoretical investigations at time-dependent density functional theory (TD-DFT) level, including state-specific (SS-PCM) solvation effects [26,27] and vibronic structure computations [28–30], were used systematically to gain insights into the nature and the energetics of the lowest excited states in unsubstituted (aza)indolizines, whereas specific and nonspecific effects induced by various functional groups were investigated comparatively in several test cases. Experimental studies by steady-state and time-resolved (TCSPC) fluorescence spectroscopy, and also a brief organic synthesis stage followed by X-ray diffraction experiments were used to validate (or infirm) several hypotheses derived theoretically.

In the PhD thesis summarized herein, following the introductory remarks (Chapter I) and a description of the methodology (Chapter II), the original contributions are organized in four main chapters, as following.

## Chapter III - Effects of substitution on the lowest excited states of pyrrolo[1,2-*b*]pyridazine

A first comparative study on two pyrrolo[1,2-*b*]pyridazine (PP) derivatives, described in chapter III, attempts to elucidate the detrimental effect of the benzoyl group on fluorescence emission, following the experimental observation emphasized by Zbancioc et al. in a recent work [17]. In spite of the apparent similarities in their absorption characteristics, fluorescence quantum yields of the two derivatives (Figure 2) are 0.80–0.90 in the case of **PP2e** and about 0.07 in the case of **PP2b**. TD-DFT computations were performed for the two molecules

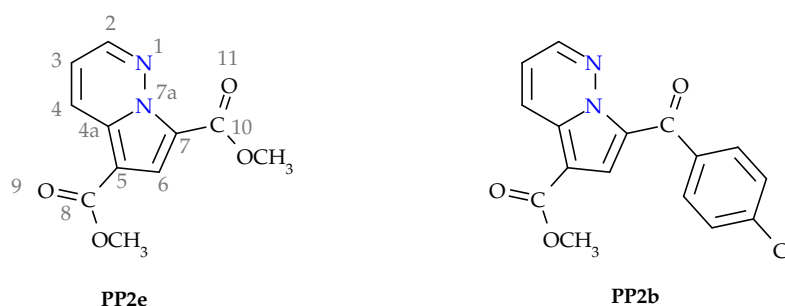


**Figure 2** – Structures of the two derivatives of PP investigated in chapter III

to unravel the origin intrinsic quenching of fluorescence in **PP2b**. In addition, steady-state absorption, excitation and fluorescence spectra needed to supplement the experimental picture, were recorded in three aprotic solvents. The lowest excited singlet **PP2e** analogue, given its simpler structure, was subjected to extensive benchmarks using the B3LYP [31] (20% Hartree–Fock exchange energy, HFx), PBE0 [32] (25% HFx), CAM-B3LYP [33] (range-dependent HFx), BH&HLYP (50% HFx) and M06-HF (100% HFx) hybrid exchange–correlation density functionals, as well as the configurational interaction singles (CIS) post Hartree–Fock method.

In the vertical approximation, the first excitation energy is overestimated by all the methods employed, B3LYP being apparently the best density functional to reproduce the position of the first absorption maximum. At the same level, fluorescence emission energy is underestimated. Upon modeling the vibronic structure of fluorescence spectrum and the first two ( $\pi \rightarrow \pi^*$ ) absorption bands (see Figure 3), the further step toward a meaningful (physical) description of the absorption phenomenon, the best overall performances are achieved using the PBE0 functional instead of the widely-used B3LYP, the apparent performances of the latter in vertical excitation energy resulting most likely from errors cancellation. Between the two, the former (PBE0, parameter-free) was hence preferred

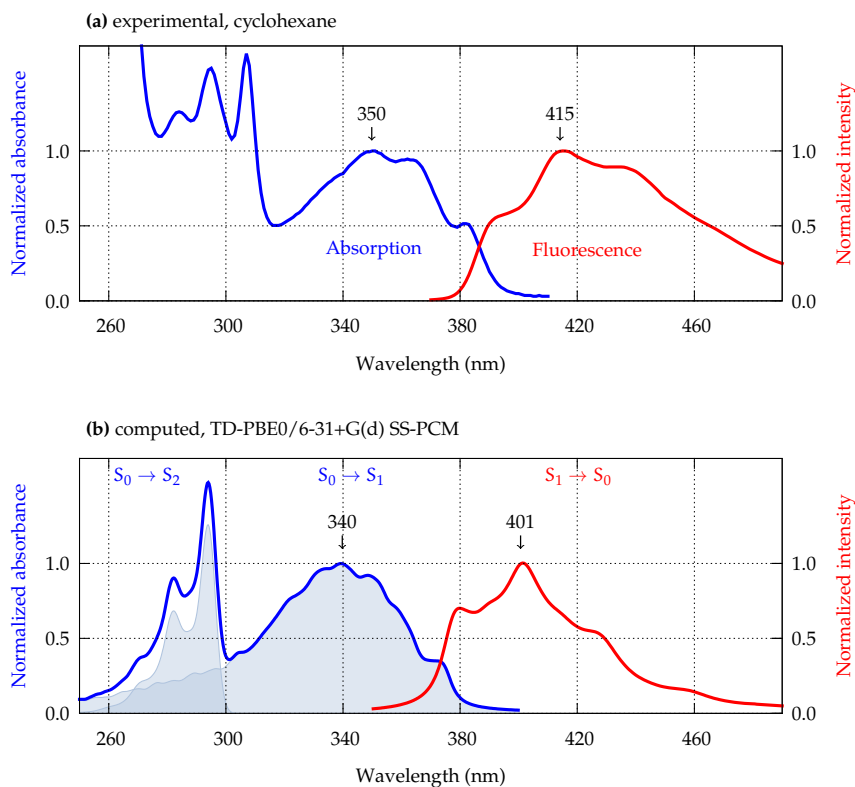


**Figure 3** – Computed vs. experimental absorption and fluorescence spectra of **PP2e**

to the latter (B3LYP, adjustable parameters, fitted) thoroughly in the subsequent works.

The same (PBE0) global hybrid density functional and also the CAM-B3LYP range-separated hybrid foresee for **PP2b** in cyclohexane a  $n\pi^*$  excited singlet below the lowest  $\pi\pi^*$ . The result may relate to the proximity of carbonyl (O) and diazine nitrogen ( $N_1$ ) lone pairs in the ground state (GS) of the most stable conformation at  $C_7$  and could explain the low fluorescence emission reported experimentally. Given the small  $\pi\pi^*$ - $n\pi^*$  energy difference in Franck-Condon (FC) region, as reproduced consistently by the two functionals, fluorescence emission may occur from the lowest vibrational levels of the allowed singlet ( $\pi\pi^*$ ) whereas excitations to upper vibronic states should trigger  $\pi\pi^* \rightarrow n\pi^*$  internal conversion (IC). Experimental excitation spectra show maxima in the long-wavelength shoulder of the first (mixed,  $n \rightarrow \pi^* + \pi \rightarrow \pi^*$ ) absorption band. One may expect hence an increase in the emission intensity when passing from nonpolar (cyclohexane) to polar (i.e. chloroform or acetonitrile), subsequent to a destabilized  $n\pi^*$  state in the latter media. Indeed, TD-DFT predicts consistently the interchange of the lowest singlets ( $n\pi^* > \pi\pi^*$ ) in polar solvents, and the long-wavelength shoulder in the recorded spectra is blue-shifted and vanishes in acetonitrile. However, excitation spectra show negligible variation with solvent

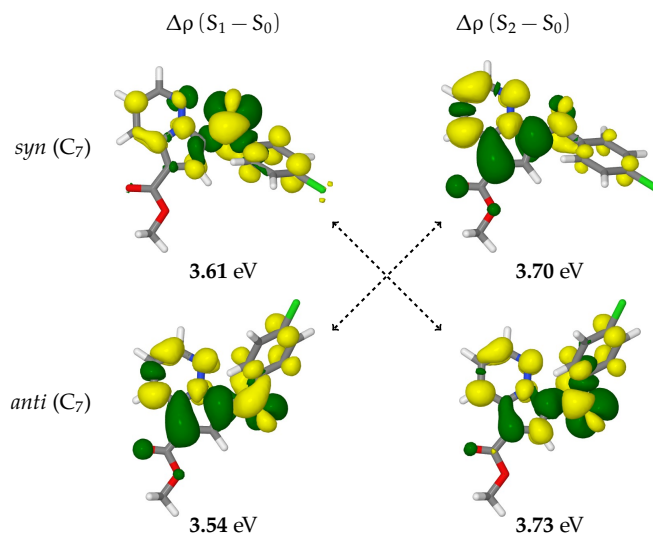


**Figure 4** – Excitation energy and character of the lowest two excited singlets of the *syn* (left) and *anti* conformers of **PP2b** depicted by electron density differences

polarity, while fluorescence emission decreases substantially in polar solvents. In the same assumption on the proximity of carbonyl and diazine nitrogen lone-pairs – in a *syn* orientation of the former (facing the heterocycle) – that stabilizes the lowest  $n\pi^*$  singlet, one may anticipate a conformational-dependent picture of the lowest excited states with respect to the benzoyl group at C<sub>7</sub>. TD-DFT foresee, by most of the functionals used herein (except M06-HF), a reversed order of the two states in the conformer having the aromatic carbonyl from C<sub>7</sub> oriented in opposite direction (*anti*), see Figure 4.

The energy of vertical excitation to the lowest ( $\pi\pi^*$ ) singlet state of the minor (*anti*) conformer falls below the lowest ( $n\pi^*$ ) state of the major (*syn*) conformation of **PP2b** and the corresponding  $S_0 \rightarrow S_1$  ( $\pi \rightarrow \pi^*$ ) transition may be tentatively assigned to the longer-wavelength shoulder of the first broad absorption band. Comparison with the excitation spectrum shown in Figure 5 (left) suggests that absorption of radiation leading to fluorescence emission occurs in the minor (*anti*) conformation, whereas the major conformer is trapped into its dark (nonradiative)  $n\pi^*$  state either by direct absorption (unlikely, due to the forbidden character) or via an efficient IC mechanism from the populated  $\pi\pi^*$  upper state, close in energy.

Theoretical results indicate that different orientations of the ester group from C<sub>5</sub> do not alter significantly the energetics or the character of the lowest excited states. The same conclusion holds for both functional groups of the highly-fluorescent **PP2e**.

Two ES minima could be located for **PP2b**, one featuring a *syn* quasi-planar orientation of the aromatic carbonyl and corresponding to the  $n\pi^*$  singlet (low-

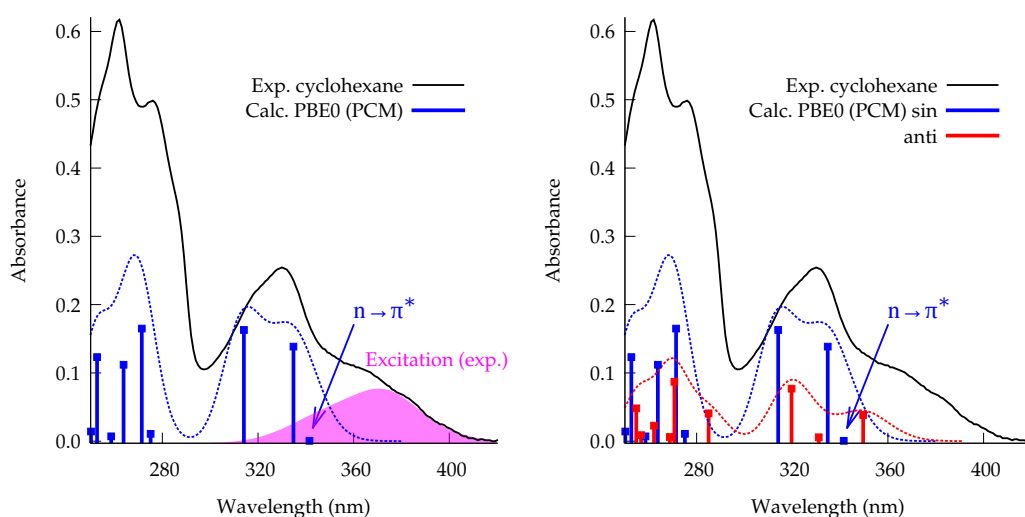


**Figure 5** – Experimental absorption spectrum of **PP2b** and computed vertical excitation spectrum considering only the major conformation (left) and both conformers at  $C_7$  (right)

est in energy at the GS geometry of the major conformer), the other having the **PP** and benzoyl fragments oriented at  $\sim 90^\circ$  in a twisted intramolecular charge transfer ES (TICT). Based on experimental evidences (strong red-shift in polar solvents), fluorescence emission has been assigned to the (TI)CT which is accessible from the GS of the minor (*anti*) conformer of **PP2b**. Despite of the

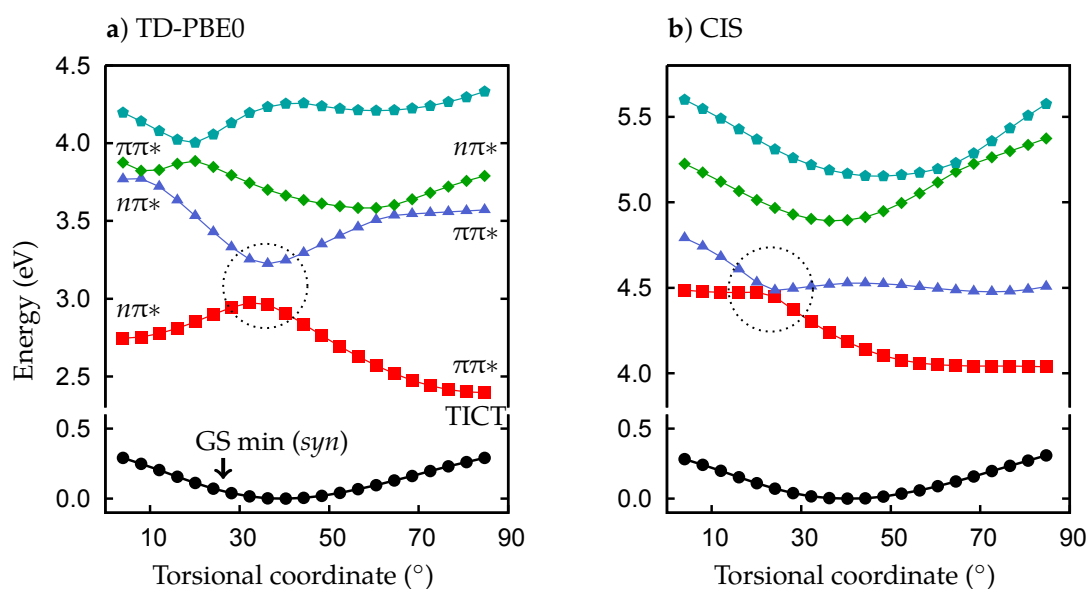


**Figure 6** – Energy of the lowest singlet ES of **PP2b** on the path leading from  $n\pi^*$  (small angles) to  $\pi\pi^*$  (TICT) minima computed at TD-PBE0 (a) and CIS (b)

severely underestimated emission energies at PBE0 level (up to 1 eV compared to experiment), the conformational dependent qualitative picture of the two lowest excited states is consistent at the PBE0, CAM-B3LYP and CIS levels (see



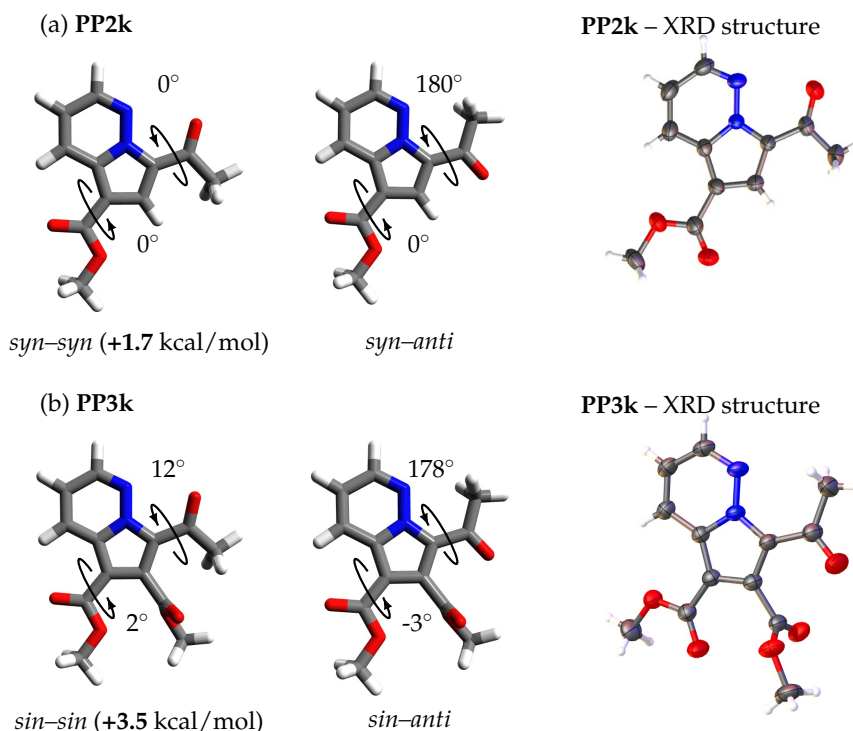


**Figure 8** – Computed (left) and experimental (right) GS geometries of acetyl-PPs

as most stable in GS for both molecules. Computed internuclear distances are in excellent agreement (r.m.s. 0.007 Å) with experimental counterparts determined from X-ray diffraction (XRD) experiments, whereas the conformational preference of the acetyl group at C<sub>7</sub> is reproduced by computations apparently only in **PP3k** (see Figure 8).

In the case of **PP2k**, qualitative discrepancies between theoretical results, predicting systematically a *syn* > *anti* energy order, and experimental evidences suggesting the opposite should reside in strong intermolecular interactions suggested to occur in the more compact crystal packing. Namely,  $\pi$ - $\pi$  interactions (at about 3.5 Å interplanar spacing, measured) and intermolecular H-bonding may prevail over intramolecular effects in dictating the conformation of **PP2k** in solid state, while the opposite is suggested by the less-compact packing of **PP3k**. Nevertheless, the two different orientations of the acetyl group in the experimental geometry of **PP2k** and **PP3k** represent a strong indication that conformational isomerism occurs at C<sub>7</sub>.

For the *anti* conformer of both **PP2k** and **PP3k**, TD-PBE0 and TD-CAM-B3LYP predict a  $\pi\pi^*$  character of the lowest singlet excited state ( $S_1$ ), separated by up to 0.30 eV from the lowest  ${}^1n\pi^*$  ( $S_2$ ) in gas phase and nonpolar solvent (cyclohexane). At the same theory level, energy ordering of the lowest two singlets is interchanged in *syn* conformation ( ${}^1n\pi^* < {}^1\pi\pi^*$ ). For **PP2k**, a state-

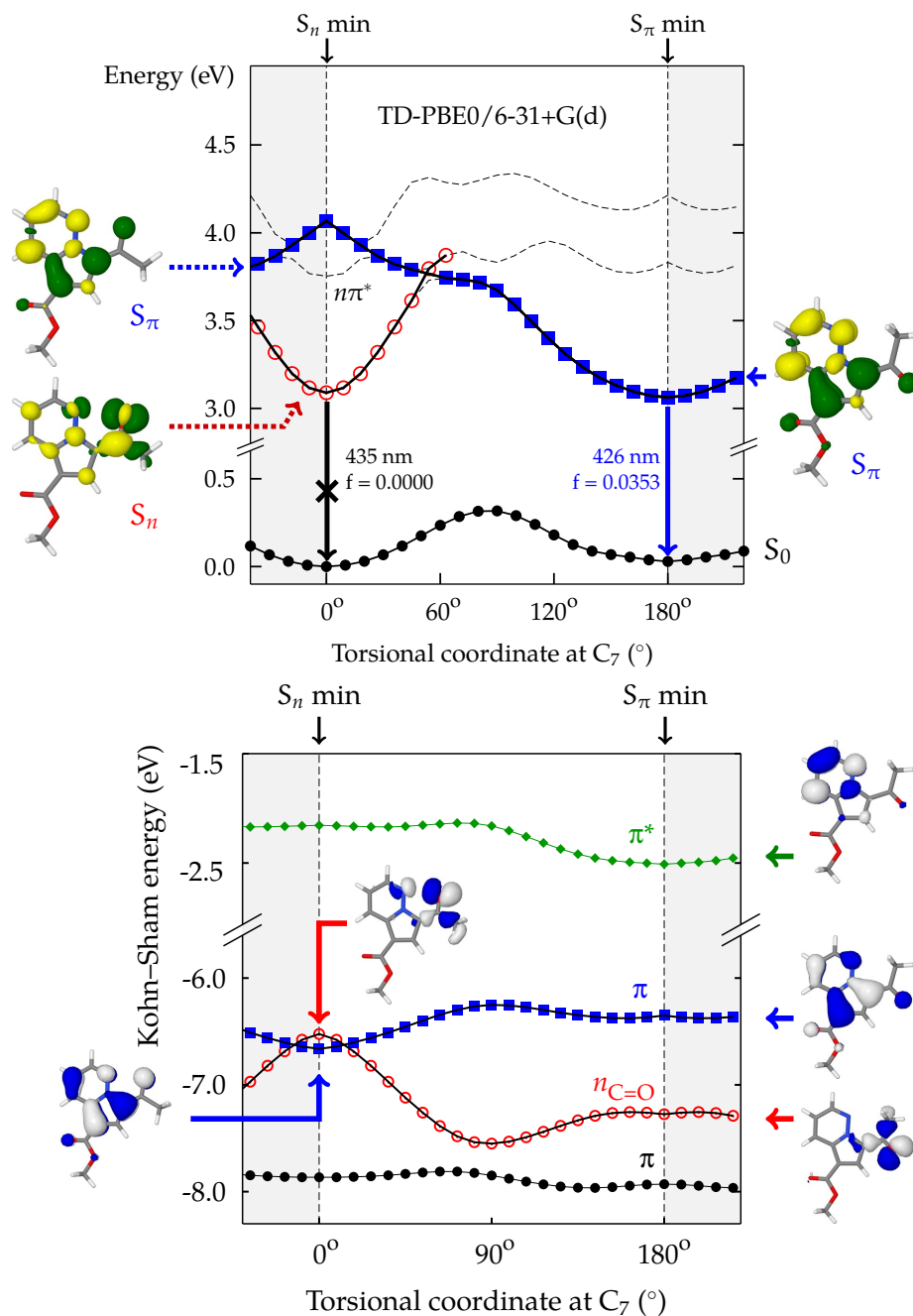


**Figure 9** – Energy of the lowest excited states of **PP2k** on the linear interpolated path between  $n\pi^*$  and  $\pi\pi^*$  equilibrium geometry (top) and frontier molecular orbital energies on the same path (bottom)

crossing is located, on the linear interpolated path between the two  $S_\pi$  ( $\pi\pi^*$ ) and  $S_n$  ( $n\pi^*$ ) minima, in a geometry having the acetyl group at 50–60° with respect to the heterocycle (see Figure 9), i. e. between the GS minimum of the *syn* conformer and the transition state for conformational interconversion (90°). As shown in Figure 9, the lowest two excited singlets are strongly influenced by the orientation of the carbonyl group at  $C_7$ , the excessive stabilization of the  $n\pi^*$

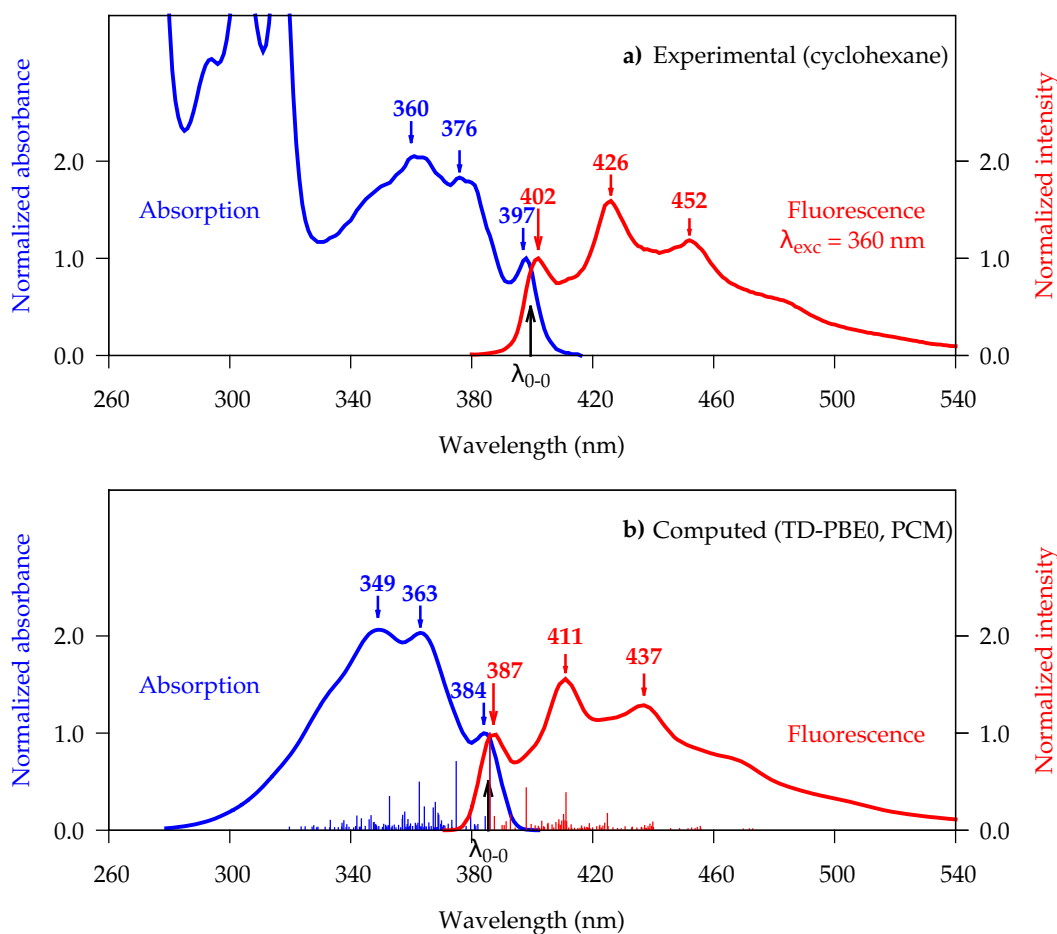


**Figure 10** – Experimental (top) and computed including the vibronic structure (bottom) absorption and fluorescence spectra of **PP2k** in cyclohexane

state at lower torsional angles (*syn*) originating from a sudden increase in the energy of a lone-pair orbital contributed from carbonyl oxygen and the nitrogen atom. According to the conformational-dependent picture of the lowest excited singlets, absorption and fluorescence spectra of **PP2k** in cyclohexane should originate from the  $\pi \rightarrow \pi^*$  transition of the major *anti* conformation (see Figure 10), whereas the proximity of the second ( $n\pi^*$ ) singlet may impact on the emission intensity. Measured fluorescence quantum yields of **PP2k** (0.24) and **PP3k** (0.25) upon excitation at 360 nm, lower than reported for their ester analogues but significantly higher than those of benzoyl-PPs and other carbonyls [35] rationalize with the abundance, at GS equilibrium, of the emitting conformer.

In polar solvents (incl. dichloromethane), both *syn* and *anti* conformers feature a  $\pi\pi^* < n\pi^*$  order of the lowest singlet, but different energy separation between the two (0.27 and 0.33, respectively) and hence different emission efficiencies due to the proximity effect. Time-resolved experiments on **PP2k** in dichloromethane reveal unambiguously a biexponential decay. Photophysi-

cal parameters determined from TCSPC curves ( $k_r = 3.3 \times 10^7 \text{ s}^{-1}$  and  $\tau_r = 30 \text{ ns}$ ) compares well with data previously reported for unsubstituted (aza)indolizines [11].

## Chapter V - Comparative investigation of the lowest electronic transition in indolizine and azaindolizines

The energetics and the character of lowest excited states in indolizine (**I**) and the seven azaindolizines 1–3 and 5–8 shown in Figure 11 were revisited in a *first-principles* theoretical approach to specifically address the second hypothesis outlined in Chapter III, namely the ICT from **PP** to aromatic carbonyls, but also to shed light on nonspecific effects from electron-withdrawing/donating groups on the first excitation energy.

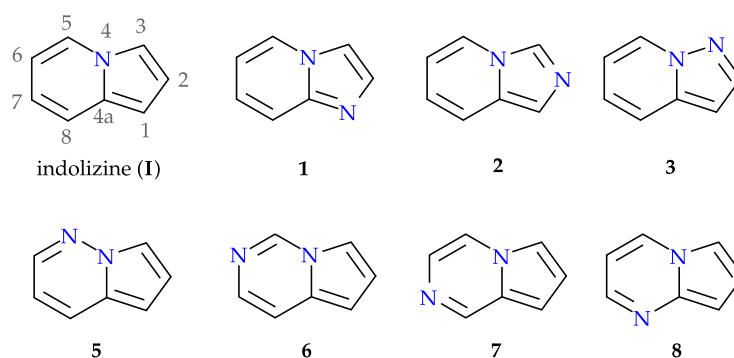


**Figure 11** – Indolizine (**I**) and the seven azaindolizines.

TD-DFT (using the B3LYP, PBE0 and CAM-B3LYP density functionals) was employed subsequently (i) in the vertical approach and (ii) modeling the vibronic structure of the first absorption/emission band, both steps being performed in vacuum and in SS-PCM solvent. In an attempt to augment the sparse experimental data with theoretical (*ab initio*) reference values, vertical excitation energies were also computed in the multiconfigurational complete active space self-consistent field (CASSCF) approach and corrected for dynamic correlation at CAPST2 level. In CASPT2//CASSCF, a full  $\pi$ -electron active space (10 *electrons*, 9 *orbitals*) was considered for indolizine, the lone pair orbital contributed from the additional nitrogen being included in the (12*e*,10*o*) active space for each of the azaindolizines.

Among the functionals considered, comparison of TD-DFT vertical excitation energies with CASPT2 reference counterparts apparently recommend the B3LYP (smallest deviations) in modeling the spectra. Compared to experimental (from

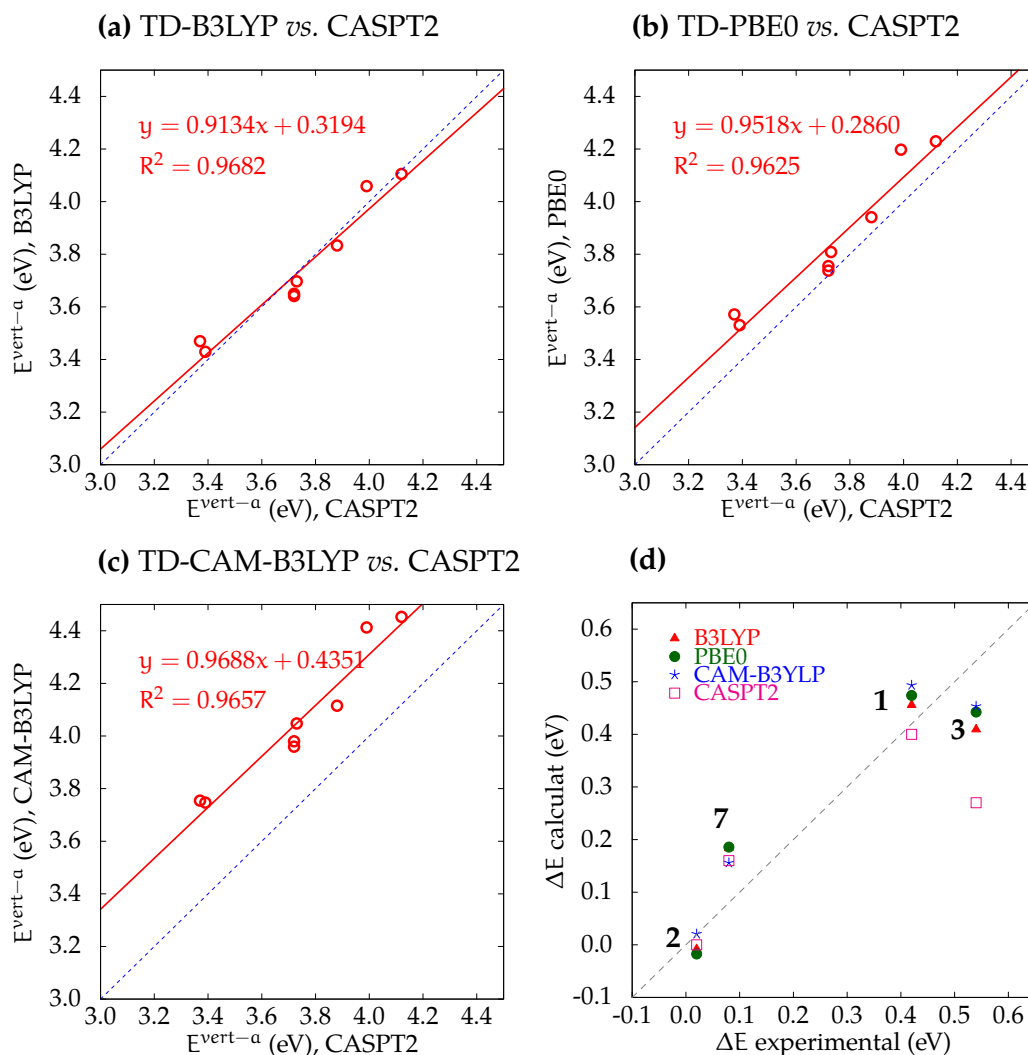


**Figure 12** – TD-DFT vs. CASPT2 (a–c) and both against available experimental spectral shifts of the first absorption band in azaindolizines compared to indolizine (d)

wavelengths of absorption maxima), both TD-DFT and CASPT2 approaches not only overrate excitation energies, but are even unable to reproduce most of the observed trends, i.e. the blue-shift of the first band in **3** compared to **1**, see Figure 12 (d). Including implicit solvent effects (PCM) does not improve the results for the lowest excitation energy, in agreement with experiments that indicate negligible effects of nonpolar solvents (*n*-hexane, cyclohexane) on the lowest excitation energy (see Refs. [10] and [9]).

In a further step, the (first) absorption and fluorescence band shapes were modeled in the FC approximation, using vibrational frequencies and normal modes computed at DFT/TD-DFT level for GS/ES. Comparison with available accurate experimental data [10] for **1** in gas-phase allowed first to assess the performances of the B3LYP, PBE0 and CAM-B3LYP density functionals in

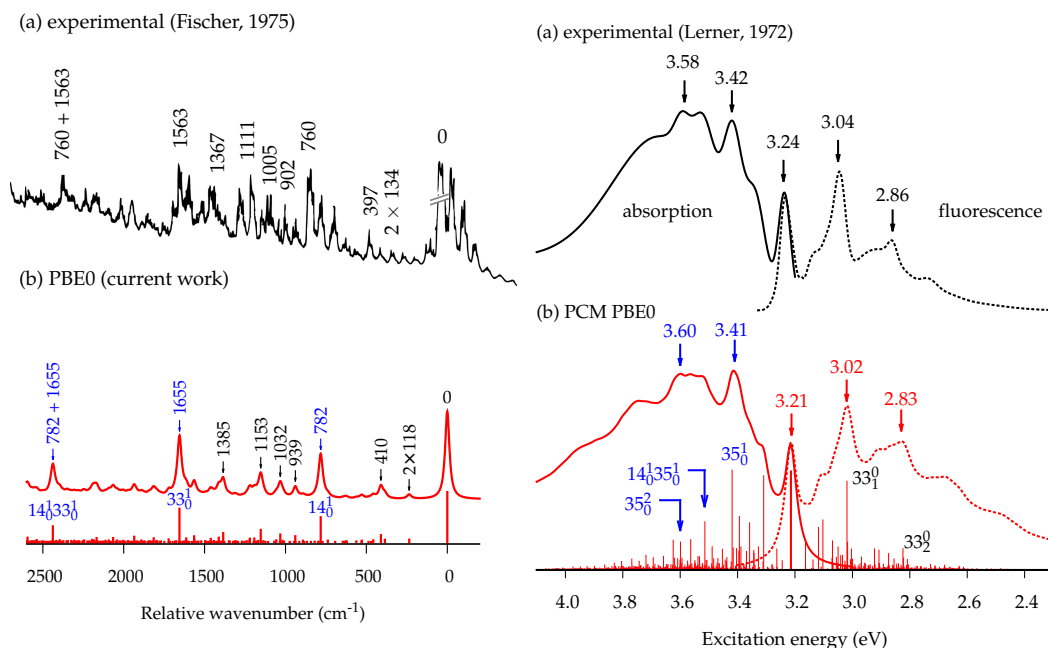


**Figure 13** – Computed [TD-PBE0/6-311+G(d,p), (b)] vs. experimental (a) vibronic structure of the first absorption and fluorescence bands of **1** in gas-phase (left, relative to band origin) and indolizine in cyclohexane (right)

reproducing separately the 0-0 energy for the first singlet transition and the vibrational frequencies in ES (expressed as wavenumbers), respectively.

In the harmonic oscillator approximation, the latter (vibrational frequencies) are overrated systematically (see Figure 13, left), that allowing to derive scaling factors for ES vibrational frequencies via a least-squares fit, whereas the "pure" electronic (adiabatic) ES-GS energy difference is substantially underestimated/overestimated by B3LYP/CAM-B3LYP.

Overall, PBE0 gives the best quantitative results among the functionals considered, with errors in 0-0 energies limited to about 0.05 eV and as low as 0.02 eV (for indolizine and **2**), values substantially lower than the observed (or predicted) changes induced by azasubstitution, namely a strong blue-shift observed/predicted in **1** and **3** and a red-shift foreseen in **5** and **8** compared to indolizine.

Seeking a rational description of these trends, that would allow further predictions on the effects of substituents, photoinduced reorganization of electron density was analyzed using CT descriptors  $q_{CT}$  (amount of transferred charge),  $d_{CT}$  (distance to CT) and  $\mu_{CT} = q_{CT} \times d_{CT}$  (CT dipole) computed from electron density differences,  $\Delta\rho^{ES-GS}$ , between the first ES and GS and recently defined [36] as:

$$q_{CT} = \int \rho_+(\mathbf{r}) \, d\mathbf{r} = - \int \rho_-(\mathbf{r}) \, d\mathbf{r} \quad (1)$$

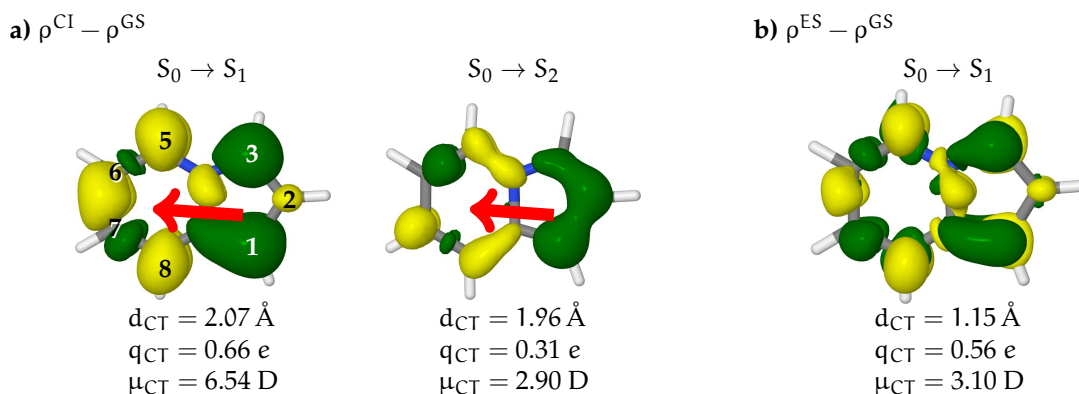


**Figure 14** – ES-GS electron density differences (a) in the first two excited singlets of indolizine computed from unrelaxed one-particle density and (b) for the first excited singlet of indolizine considering the relaxed ES electron density

and

$$d_{CT} = |R_+ - R_-| = \left| \frac{\int \mathbf{r} \cdot \rho_+(\mathbf{r}) \, d\mathbf{r}}{\int \rho_+(\mathbf{r}) \, d\mathbf{r}} - \frac{\int \mathbf{r} \cdot \rho_-(\mathbf{r}) \, d\mathbf{r}}{\int \rho_-(\mathbf{r}) \, d\mathbf{r}} \right| \quad (2)$$

where

$$\rho_+(\mathbf{r}) = \begin{cases} \Delta\rho(\mathbf{r}), & \Delta\rho(\mathbf{r}) > 0 \\ 0, & \Delta\rho(\mathbf{r}) < 0 \end{cases}, \quad \rho_-(\mathbf{r}) = \begin{cases} 0, & \Delta\rho(\mathbf{r}) > 0 \\ \Delta\rho(\mathbf{r}), & \Delta\rho(\mathbf{r}) < 0 \end{cases} \quad (3)$$

Density reorganization in the first ES of indolizine (see Figure 14) and azaindolizines reflect an overall CT from the pyrrole to the (di)azine ring. In spite of strong influences induced by azasubstitution simultaneously on the magnitude and orientation of GS and ES dipole moments, the effects on the first excitation energy could not be rationalized in terms of CT dipole,  $\mu_{CT} = |\vec{\mu}^{ES} - \vec{\mu}^{GS}|$  (arrow shown in Figure 14), or  $d_{CT}/q_{CT}$ . Quantitative descriptors described above do not account for individual (atomic) contribution to the CT, namely the multipolar CT character. As shown in Figure 14, four of the seven centers of indolizine susceptible to (aza)substitution participate to different extents in the CT either as donors (1 and 3) or acceptors (2, 5 and 8), whereas the remaining two (6 and 7) are marginally involved. Essentially the same qualitative conclusion arise when interpreting electron density differences computed from relaxed (Figure 14, b) instead of the approximate (unrelaxed) one-particle ES density (Figure 14, a).

In the simpler (approximate) approach, all the three CT descriptors derived from electron densities (computed by subtracting GS total density from one-particle ES density) are reproduced by ES-GS differences in Mulliken partial

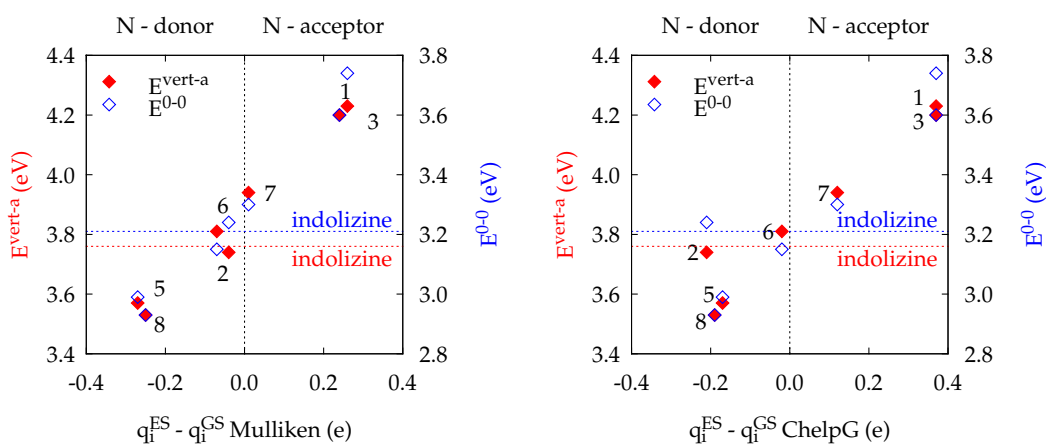


**Figure 15** – Vertical excitation energies (left axis) and 0–0 energies (right axis) vs. ES-GS differences in partial atomic charges in the parent indolizine at the center of azasubstitution: (a) differences in Mulliken charges using the unrelaxed ES density and (b) differences in ChelpG charges using the relaxed ES density

atomic charges,  $\delta q_i = q_i^{\text{ES}} - q_i^{\text{GS}}$  in a discrete variant of the formalism given in Eqs. (1) and (2). In indolizine, centers 1 and 3 qualify with similar quantitative extents as donors ( $\delta q_i > 0$  or  $q_i^{\text{ES}} > q_i^{\text{GS}}$ ), whereas 2, 5 and 8 ( $\delta q_i < 0$ ) involve as acceptors in the photoinduced CT. For centers 1, 2, and 3, the semi-quantitative correlation of the first excitation energy of the corresponding azaindolizine with the amount of charge transferred from (in 1 and 3) or to (in 2) the corresponding center confirms the previous semiempirical systematics proposed by Evleth [22]. Current (non-empirical TD-DFT) results extend the same rationalization to azaindolizines **5** and **8** (see Figure 15, a). The correlation pertains (see Figure 15, b) when the relaxed (instead of unrelaxed, one-particle) ES density is considered, except that in this case differences in ChelpG charges (instead of Mulliken) recover with acceptable accuracy the CT indices derived from electron density.

Except the centers 2, 6 and 7, for which the correlation seems inconsistent between the two approaches, the effect of various electron-withdrawing/donating groups on the energy of the lowest excited state may be rationalized in the same manner.

Deviations of data plotted in Figure 15 from a straight line may relate to the fact that in actual azaindolizines the computed ES-GS absolute differences in partial atomic charges (in both point charge models) are substantially lower than in the parent indolizine. Namely in **1** and **3** / **5** and **8**, the additional nitrogen atom in the pyrrole ring involves as donor/acceptor in the CT with a lesser extent than the corresponding carbon atom from the parent indolizine. The blue/red shift of the first absorption band in (aza)indolizines bearing ester/amine groups

on the pyrrole ring in positions adjacent to the bridge confirm the conclusion above.

## Chapter VI - Structure and spectral properties of some isoindolo-diazines

Polycyclic diazines shown in Figure 16 (also referred to as isoindolo-diazines) were evaluated in two parallel investigations aiming toward (i) an assessment of their biologic activity and (ii) testing the hypothesis of a photoinduced CT from the pyrrole ring (or the entire PP) to the aromatic carbonyl fragment. In

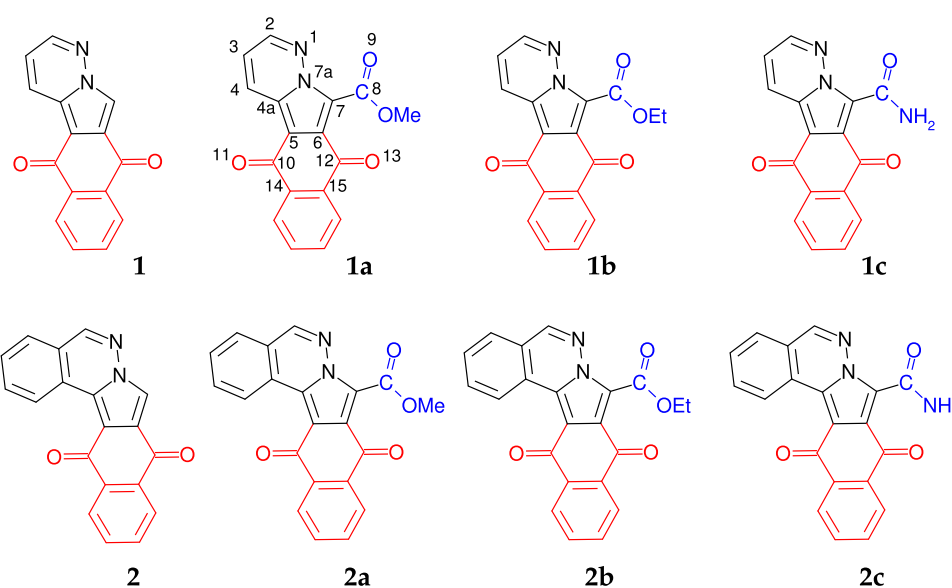


**Figure 16** – Structures of polycyclic pyrrolo-diazines with aromatic carbonyl groups

the former approach, the anticancer activity of compounds **1a-c** and **2a-c** was tested *in vitro* against Leukemia CCRF-CEM, Leukemia MOLT-4, Non-Small Cell Lung Cancer NCI-H460, and Breast Cancer MCF7 cells. All the compounds have significant anticancer activity, expressed by the Percentage Growth Inhibition (PGI) factor, the pentacyclic systems (**2a-c**) showing the largest values. A plausible hypothesis formulated [37] to explain the observed biological properties designated the compounds as DNA intercalators, relying on the coplanar molecular geometry of the four(five) condensed rings as proved by XRD experiments [38,39] regardless the substituent on the remaining position of the pyrrole ring (see Figure 17).

Regarding the influence of the extended  $\pi$ -subsystem on the photophysical properties, structures **1a-c** may be ascribed as PPs bearing aromatic carbonyl groups (at the pyrrole ring) that are constrained to adopt coplanar orientation

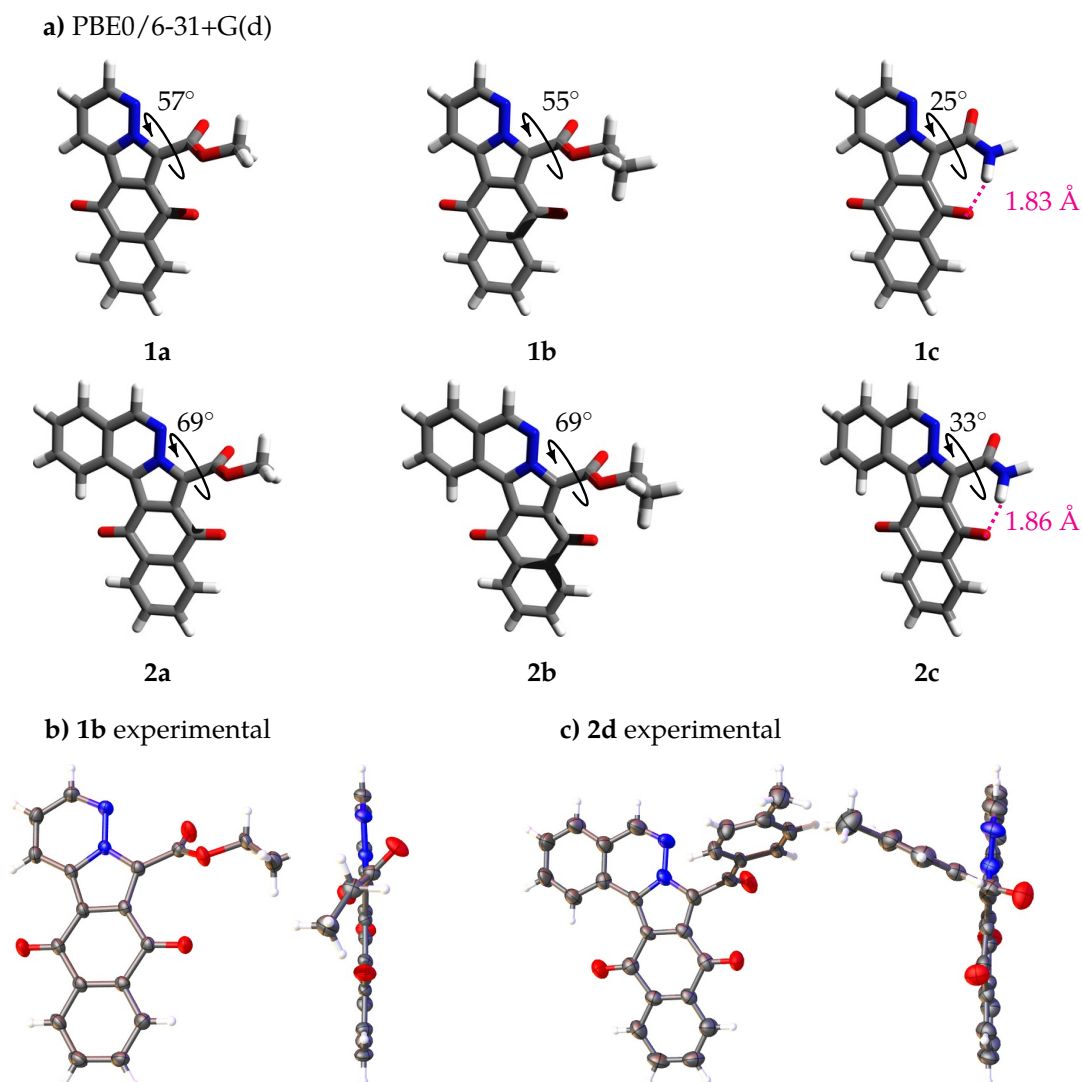


**Figure 17** – Molecular geometry (a) computed for compounds **1a-c** and **2a-c** and (b) determined by XRD for **1b** and **2d**

with respect to the **PP** rings. Consequent to an extended electron delocalization, the first absorption band of all the isoindolo-diazines investigated is red-shifted toward the visible region (410-420 nm).

TD-DFT computations using the PBE0 and CAM-B3LYP functionals foresee in the first ES a photoinduced CT from the **PP** (**PH**) to the quinone fragment via the pyrrole ring. Given the small energy separation between the lowest ( $\pi\pi^*$  and  $n\pi^*$ ) excited singlets in **1a** and **1b**, plots of electron density differences reveal a mixed ( $\pi\pi^*+n\pi^*$ ) character of the lowest ES (see Figure 18). In contrast, the first ES in **1c** and **2c** (bearing amine group on the pyrrole ring) has pure  $\pi\pi^*$  character. Assuming a proximity effect, the predictions correlate with measured fluorescence quantum yields, substantially higher in the case of **1c** (> 60%) than in **1a,b** (< 20%).

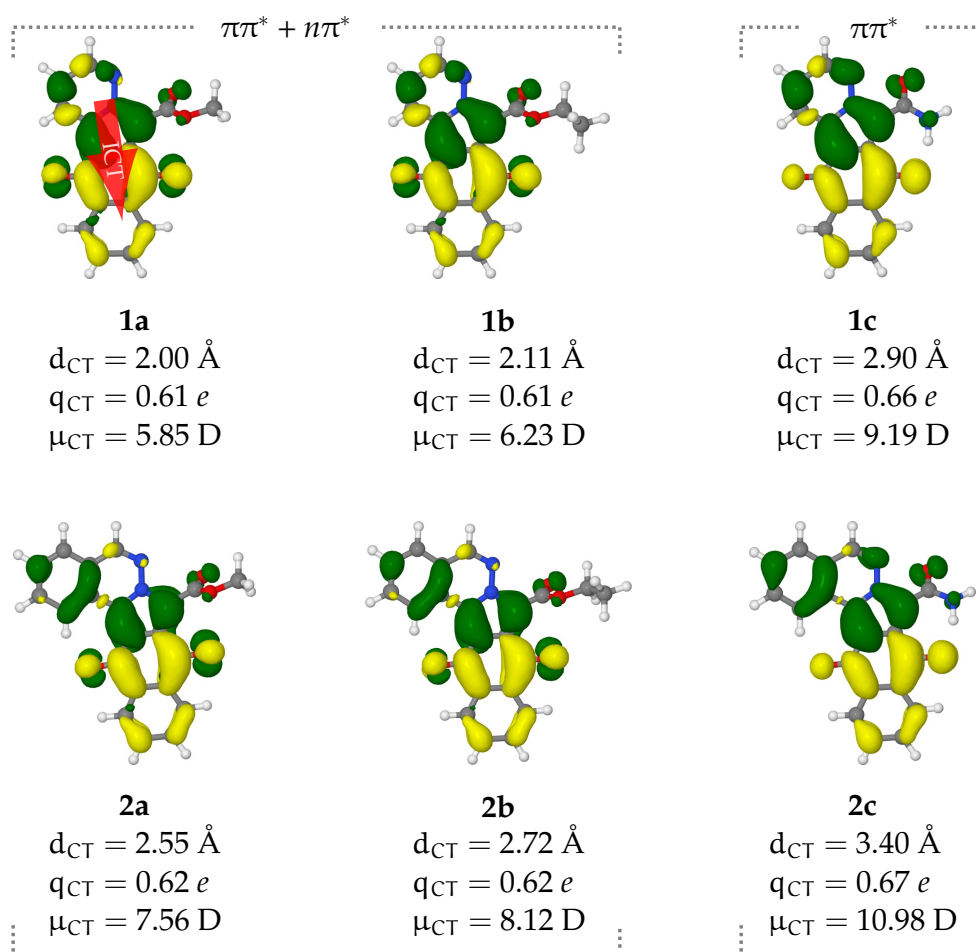


**Figure 18** – Electron density difference and CT descriptors for the lowest excited singlet of **1a-c**

Compared to the corresponding unsubstituted four-rings system **1** (quantum yield about 40% [40]) the two opposite trends may be unequivocally assigned to the substituent on the pyrrole ring: the ester group has a detrimental effect whereas the amino group enhances the fluorescence emission. Even in a pre-twisted orientation, the former is expected to stabilize the lowest  $n\pi^*$  singlet ( $S_2$ ) by destabilizing the lone pair from either aromatic carbonyl or the pyridazine nitrogen, depending on the conformation adopted in GS. For the lowest excited singlets of **1a**, TD-DFT predicts an interchange of the major character ( $\pi\pi^* \leftrightarrow n\pi^*$ ) in both nearly-planar orientations.

In the case of **1c** (**2c**), the pure  $\pi\pi^*$  character of  $S_1$  and consequently an increased fluorescence intensity may originate from one of the following effects of an intramolecular hydrogen bond suggested by GS equilibrium geometry (see Figure 17): (i) a stabilization of carbonyl lone-pair orbital, and hence an increase in the energy of the lowest  $n\pi^*$  singlet and (ii) a stabilization and enhancement

of the first (ICT) state, the adjacent aromatic carbonyl involved in the hydrogen bond playing as acceptor in the photoinduced CT. Comparison in computed

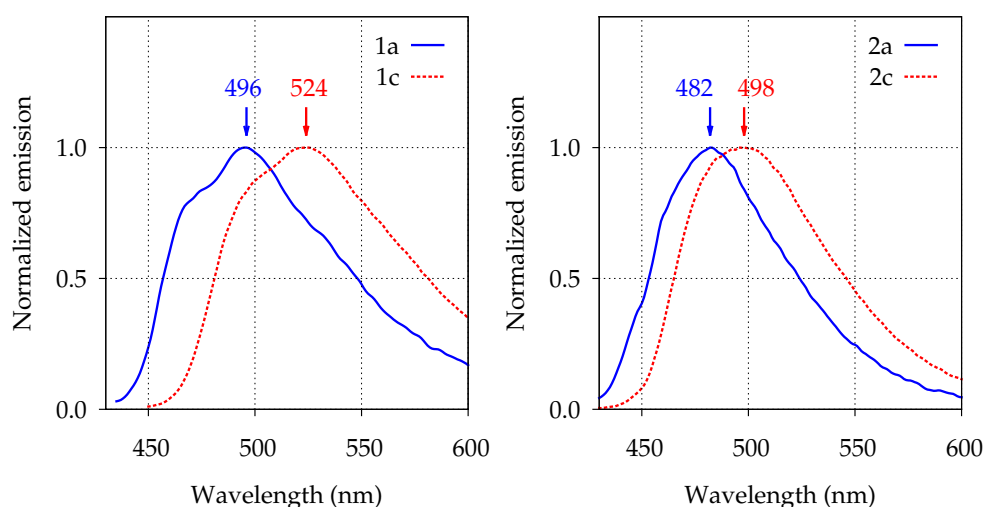


**Figure 19** – Experimental fluorescence spectra of **1a,c** and **2a,c** recorded in dichloromethane

excitation and emission energies (TD-DFT) and red-shifted absorption and fluorescence bands of **1a** (compared to **1a,b**) and **2c** (compared to **2a,b**), see Figure 19, add theoretical and experimental support for the latter. Namely, intramolecular hydrogen bonds involving aromatic carbonyls enhance and induce a red-shift on fluorescence emission by stabilizing the ICT state. Intermolecular interactions with molecules of biological interest (such as nucleic acids), mostly consisting of H-bonds, are expected to induce similar effects. That opens the route for a reliable spectroscopic approach in investigating non-bonding interactions involved in the biological activity of these systems.

## General conclusions

The lowest singlet transition in (aza)indolizines is reproduced, at unprecedented accuracy for unsubstituted systems, by TD-DFT using the parameter-free PBE0 density functional using a basis set with moderate complexity. At the same theory level, spectral shifts induced by various groups are reproduced with errors lower than reported in most of the previous works by other authors. Current results recommend this functional/basis set combination in modeling the (lowest) valence singlet transitions in (aza)indolizine derivatives. Particular aspects related to large aromatic groups featuring torsional degrees of freedom and specific solvation effects require additional investigations (i.e. at CAM-B3LYP level).

Excitation to the lowest ES in (aza)indolizines triggers an electron density reorganization (charge transfer) between the two fused rings. Each of the three and four centers of the two rings contribute with different extent either as donor or as acceptor, yielding a multipolar CT character. The first excitation energy in azaindolizines, computed in either the vertical approach or upon modeling the vibronic structure (the latter being strongly required for a reliable comparison with experimental data) correlate qualitatively with ES-GS differences in partial atomic charges computed for the center of indolizine corresponding to azasubstitution. Results presented herein not only confirm a previous systematics proposed for 1-, 2- and 3-azaindolizine (based on heavily-parametrized semiempirical results) but allow the same model to be applied for 5- and 8-azaindolizine as well as for describing/predicting nonspecific effects (of electron-withdrawing/donating groups) on the first excitation energy.

In the case of **PP**, the functional group on the pyrrole ring (adjacent to the bridgehead nitrogen atom) influences not only the CT ( $\pi\pi^*$ ) state, but also stabilizes the lowest  $n\pi^*$  singlet. In effect, a functional group featuring lone-pairs (such as carbonyl) may impact, depending on its orientation with respect to the pyridazine ring, on fluorescence emission.

In isoindolo-diazine systems, the relative energy of the lowest two singlets,  $\pi\pi^*$  and  $n\pi^*$ , strongly depends on the substituent on the remaining position on the pyrrole ring. The former (emitting) state features a strong ICT, from the pyrrole ring to the quinone fragment, that may be enhanced by specific intra- or inter-molecular interactions involving the carbonyl group on the acceptor side. In isoindolo-diazines bearing ester groups, the decrease in the fluorescence emission intensity relate to a stabilization of the lowest  $n\pi^*$  singlet and hence a proximity effect induced in both nearly-planar orientations of the additional functional group.

## Selected references

- [1] M. H. Palmer, I. C. Walker, and M. F. Guest, *Chem. Phys.*, 1998, **238**(2), 179–199, doi: [10.1016/S0301-0104\(98\)00285-7](https://doi.org/10.1016/S0301-0104(98)00285-7).
- [2] M. N. R. Ashfold, B. Cronin, A. L. Devine, R. N. Dixon, and M. G. D. Nix, *Science (New York, N.Y.)*, 2006, **312**(5780), 1637–40, doi: [10.1126/science.1125436](https://doi.org/10.1126/science.1125436).
- [3] J. Wan, J. Meller, M. Hada, M. Ehara, and H. Nakatsuji, *J. Chem. Phys.*, 2000, **113**(18), 7853, doi: [10.1063/1.1316034](https://doi.org/10.1063/1.1316034).
- [4] M. Barbatti, J. Pittner, M. Pederzoli, U. Werner, R. Mitrić, V. Bonačić-Koutecký, and H. Lischka, *Chem. Phys.*, 2010, **375**(1), 26–34, doi: [10.1016/j.chemphys.2010.07.014](https://doi.org/10.1016/j.chemphys.2010.07.014).

- [5] I. Yamazaki, K. Sushida, and H. Baba, *J. Chem. Phys.*, 1979, **71**(1), 381, doi: [10.1063/1.438081](https://doi.org/10.1063/1.438081).
- [6] M. Klessinger and J. Michl, *Excited States and Photochemistry of Organic Molecules*, VCH, 1995.
- [7] A. Bolovinos, P. Tsekeris, J. Philis, E. Pantos, and G. Andritsopoulos, *J. Mol. Spectrosc.*, 1984, **103**(2), 240–256, doi: [10.1016/0022-2852\(84\)90051-1](https://doi.org/10.1016/0022-2852(84)90051-1).
- [8] Y. Li, J. Wan, and X. Xu, *J. Comput. Chem.*, 2007, **28**(10), 1658–1667, doi: [10.1002/jcc.20555](https://doi.org/10.1002/jcc.20555).
- [9] D. A. Lerner and E. M. Evleth, *Chem. Phys. Lett.*, 1972, **15**(2), 260–262, doi: [10.1016/0009-2614\(72\)80163-5](https://doi.org/10.1016/0009-2614(72)80163-5).
- [10] G. Fischer and R. Naaman, *J. Mol. Spectrosc.*, 1975, **57**(2), 284–293, doi: [10.1016/0022-2852\(75\)90031-4](https://doi.org/10.1016/0022-2852(75)90031-4).
- [11] D. A. Lerner, P. M. Horowitz, and E. M. Evleth, *J. Phys. Chem.*, 1977, **81**(1), 12–17, doi: [10.1021/j100516a004](https://doi.org/10.1021/j100516a004).
- [12] Y. Cheng, B. Ma, and F. Wudl, *J. Mat. Chem.*, 1999, **9**(9), 2183–2188, doi: [10.1039/a903025e](https://doi.org/10.1039/a903025e).
- [13] T. Mitsumori, M. Bendikov, J. Sedó, and F. Wudl, *Chem. Mater.*, 2003, **15**(20), 3759–3768, doi: [10.1021/cm0340532](https://doi.org/10.1021/cm0340532).
- [14] T. Mitsumori, I. M. Craig, I. B. Martini, B. J. Schwartz, and F. Wudl, *Macromolecules*, 2005, **38**(11), 4698–4704, doi: [10.1021/ma048091y](https://doi.org/10.1021/ma048091y).
- [15] G. N. Zbancioc and I. I. Mangalagiu, *Synlett*, 2006, **37**(5), 0804–0806, doi: [10.1055/s-2006-932459](https://doi.org/10.1055/s-2006-932459).
- [16] G. Zbancioc and I. I. Mangalagiu, *Tetrahedron*, 2010, **66**(1), 278–282, doi: [10.1016/j.tet.2009.10.110](https://doi.org/10.1016/j.tet.2009.10.110).
- [17] G. N. Zbancioc, T. Huhn, U. Groth, C. Deleanu, and I. I. Mangalagiu, *Tetrahedron*, 2010, **66**(24), 4298–4306, doi: [10.1016/j.tet.2010.04.050](https://doi.org/10.1016/j.tet.2010.04.050).
- [18] M. Becuwe, D. Landy, F. Delattre, F. Cazier, and S. Fourmentin, *Sensors*, 2008, **8**(6), 3689–3705, doi: [10.3390/s8063689](https://doi.org/10.3390/s8063689).
- [19] A. V. Rotaru, I. D. Druta, T. Oeser, and T. J. J. Müller, *Helvetica Chimica Acta*, 2005, **88**(7), 1798–1812, doi: [10.1002/hlca.200590141](https://doi.org/10.1002/hlca.200590141).
- [20] A. Rotaru, I. Druta, E. Avram, and R. Danac, *Arkivoc*, 2009, **2009**(xiii), 287–299.
- [21] V. Galasso, G. Alti, and A. Bigotto, *Theor. Chim. Acta*, 1968, **9**(3), 222–229, doi: [10.1007/BF00526601](https://doi.org/10.1007/BF00526601).
- [22] E. M. Evleth, *Theor. Chim. Acta*, 1970, **16**(1), 22–32, doi: [10.1007/BF01045963](https://doi.org/10.1007/BF01045963).
- [23] M. Vasilescu, R. Bandula, O. Cramariuc, T. Hukka, H. Lemmetyinen, T. T. Rantala, and F. Dumitrascu, *J. Photochem. Photobio. A*, 2008, **194**(2-3), 308–317, doi: [10.1016/j.jphotochem.2007.08.029](https://doi.org/10.1016/j.jphotochem.2007.08.029).

- [24] P. J. Aittala, O. Cramariuc, M. Vasilescu, R. Bandula, and T. I. Hukka, *Chem. Phys.*, 2009, **360**(1-3), 162–170, doi: [10.1016/j.chemphys.2009.04.020](https://doi.org/10.1016/j.chemphys.2009.04.020).
- [25] P. J. Aittala, O. Cramariuc, T. I. Hukka, M. Vasilescu, R. Bandula, and H. Lemmetyinen, *J. Phys. Chem. A*, 2010, **114**(26), 7094–101, doi: [10.1021/jp9104536](https://doi.org/10.1021/jp9104536).
- [26] R. Improta, V. Barone, G. Scalmani, and M. J. Frisch, *J. Chem. Phys.*, 2006, **125**(5), 054103, doi: [10.1063/1.2222364](https://doi.org/10.1063/1.2222364).
- [27] R. Improta, G. Scalmani, M. J. Frisch, and V. Barone, *J. Chem. Phys.*, 2007, **127**(7), 074504, doi: [10.1063/1.2757168](https://doi.org/10.1063/1.2757168).
- [28] F. Santoro, R. Improta, A. Lami, J. Bloino, and V. Barone, *The Journal of chemical physics*, 2007, **126**(8), 084509, doi: [10.1063/1.2437197](https://doi.org/10.1063/1.2437197).
- [29] F. Santoro, A. Lami, R. Improta, J. Bloino, and V. Barone, *The Journal of chemical physics*, 2008, **128**(22), 224311, doi: [10.1063/1.2929846](https://doi.org/10.1063/1.2929846).
- [30] F. Santoro and V. Barone, *International Journal of Quantum Chemistry*, 2010, **110**(2), 476–486, doi: [10.1002/qua.22197](https://doi.org/10.1002/qua.22197).
- [31] A. D. Becke, *J. Chem. Phys.*, 1993, **98**(7), 5648, doi: [10.1063/1.464913](https://doi.org/10.1063/1.464913).
- [32] C. Adamo and V. Barone, *J. Chem. Phys.*, 1999, **110**(13), 6158, doi: [10.1063/1.478522](https://doi.org/10.1063/1.478522).
- [33] T. Yanai, *Chem. Phys. Lett.*, 2004, **393**(1-3), 51–57, doi: [10.1016/j.cplett.2004.06.011](https://doi.org/10.1016/j.cplett.2004.06.011).
- [34] D. Maftei, G. Zbancioc, I. Humelnicu, and I. Mangalagiu, *J. Phys. Chem. A*, 2013, **117**(15), 3165–75, doi: [10.1021/jp311396m](https://doi.org/10.1021/jp311396m).
- [35] Y. Niko, Y. Hiroshige, S. Kawauchi, and G.-i. Konishi, *Tetrahedron*, 2012, **68**(31), 6177–6185, doi: [10.1016/j.tet.2012.05.072](https://doi.org/10.1016/j.tet.2012.05.072).
- [36] T. Le Bahers, C. Adamo, and I. Ciofini, *J. Chem. Theory Comput.*, 2011, **7**(8), 2498–2506, doi: [10.1021/ct200308m](https://doi.org/10.1021/ct200308m).
- [37] D. Mantu, D. Maftei, D. Iurea, C. Ursu, and V. Bejan, *Med. Chem. Res.*, 2013, **23**(6), 2909–2915, doi: [10.1007/s00044-013-0878-8](https://doi.org/10.1007/s00044-013-0878-8).
- [38] D. Mantu, D. Maftei, D. Iurea, and V. Bejan Antoci, *Rev. Chim.*, 2012, **63**(12), 1239–1242.
- [39] D. Maftei, D. Mantu, and V. Bejan, *Rev. Chim.*, 2013, **64**(3), 301–303.
- [40] T. Mitsumori, M. Bendikov, O. Dautel, F. Wudl, T. Shioya, H. Sato, and Y. Sato, *J. Am. Chem. Soc.*, 2004, **126**(51), 16793–803, doi: [10.1021/ja049214x](https://doi.org/10.1021/ja049214x).